Epilepsia, 51(1):98–107, 2010
doi: 10.1111/j.1528-1167.2009.02259.x

FULL-LENGTH ORIGINAL RESEARCH

Histologic and morphologic effects of valproic acid and oxcarbazepine on rat uterine and ovarian cells

***Ali Cansu, †Deniz Erdogan, ‡Ayse Serdaroglu, †Gülnur Take, §Zafer K. Coskun, and ¶Seren G. Gurgen**

***Department of Pediatric Neurology, Karadeniz Technical University Faculty of Medicine, Merkez/Trabzon, Turkey; †Department of Histology and Embryology, Gazi University Faculty of Medicine, Ankara, Turkey; ‡Department of Pediatric Neurology, Gazi University Faculty of Medicine, Ankara, Turkey; §Department of Anatomy, Gazi University Faculty of Medicine, Ankara, Turkey; and ¶School of Vocational Health Service, Celal Bayar University, Manisa, Turkey**

Summary

Purpose: To determine the histologic and morphologic effects of valproic acid (VPA) and oxcarbazepine (OXC) on rat uterine and ovarian cells.

Methods: Fifty-six female prepubertal Wistar rats (21–24 days old and weighing between 47.5 and 58.1 g) were divided equally into four groups, which were given drinking water (controls), 300 mg/kg/day of VPA, 100 mg/kg/day of OXC or VPA + OXC via gavage, for 90 days. Ovaries and uteri of rats on proestrous and diestrous phases of estrous cycle were extirpated and placed in a fixation solution. The tissue specimens were assessed with apoptosis (TUNEL) staining protocols, eosinophil counting, and electron microscopic techniques.

Results: In uteri, apoptosis in stroma, mitochondrial swelling, and cristolysis were observed in the VPA group, and OXC led to negative effects on epithelial cell and intracellular edema. In ovaries, both drugs increased apoptosis and intracytoplasmic edema. Organelle structure disruption was also observed in the OXC group. More conspicuous degenerative modifications were determined in the VPA + OXC group. In uteri, the number of TUNEL-positive luminal epithelial cells was 7.20 ± 1.32 in controls, and significantly increased to 29.60 ± 1.58, 34.20 ± 2.53, and 54.80 ± 2.04 in VPA, OXC, and VPA + OXC groups, respectively ($p < 0.001$). The highest number of TUNEL-positive glandular epithelium cells was observed in the VPA + OXC group; however, the number of TUNEL-positive stroma cells was highest in the VPA group. The highest number of eosinophils in stroma was in the VPA group.

Conclusion: VPA and OXC trigger apoptotic and degenerative effects on rat uterine and ovarian cells. VPA also prevents implantation of embryo to the uterus and causes abortion via endometrial eosinophil infiltration.

KEY WORDS: Valproic acid, Oxcarbazepine, Uterus, Ovary, Rat.

Epilepsy affects at least 50 million people worldwide, and is one of the most common neurologic disorders. Valproic acid (VPA; 2-propylpentanoic acid) and oxcarbazepine (OXC; 10,11-dihydro-10-oxo-5H-dibenz[b,f]-azepine-5-carboxamide) are prescribed antiepileptic drugs (AEDs), and it is important to know the effects of these two AEDs on cells for safe clinical use. Electron microscopic examinations give important clues about the effects of VPA and OXC at the cell level. There are studies investigating the effects of VPA on rat cerebral cortex capillaries (Vorbrodt et al., 2005), hippocampal cortex (Sobaniec-Lotowska, 2003), and embryos (Seegmiller et al., 1991); on mouse fetal and maternal organs (Emmanouil-Nikoloussi et al., 2004); and on human hepatoblastoma cells (Neuman et al., 2001) using electron microscopic techniques; however, the studies investigating the effects of OXC are limited.

Both VPA and OXC treatment have long-term negative effects on rat ovaries. Treatment with VPA or OXC from prepuberty to adulthood has apoptotic effects and causes deterioration of folliculogenesis in rat ovarian

Accepted June 2, 2009; Early View publication August 8, 2009.
Address correspondence to Ali Cansu, MD, Department of Pediatric Neurology, Karadeniz Technical University Faculty of Medicine, 61080 Merkez/Trabzon, Turkey. E-mail: acansu2003@yahoo.com

Wiley Periodicals, Inc.
© 2009 International League Against Epilepsy

follicles (Cansu et al., 2008). The aim of the present study was to determine the histologic and morphologic effects of two AEDs (VPA and OXC) on rat uterine and ovarian cells.

Materials and Methods

Animals

In this experimental study, 56 female prepubertal Wistar rats (21–24 days old and weighing between 47.5 and 58.1 g) from the Gazi University Medical Faculty Animal Laboratory were used. All animals were housed in groups in plastic cages at constant room temperature (21–22°C) and in a 12 h light–dark cycle (lights on at 07:00 a.m.). Rats had free access to food and water. All animal experiments were carried out in accordance with the European Communities Council Directive of November 24, 1986 (86/609/EEC) and were approved by the Animal Care Committee of Gazi University.

Experimental procedure and dosing

Rats were divided into four experimental groups, with 14 rats in each group. The experimental groups were as follows: group one (control group) received the control solution, group two (VPA group) received 300 mg/kg/day of VPA [Depakin (200 mg/1,000 μl solution); Sanofi Dogu, Istanbul, Turkey], group three (OXC group) received 100 mg/kg/day of OXC [Trileptal (60 mg/1,000 μl solution); Novartis, Istanbul, Turkey], and group four (VPA + OXC group) received 300 mg/kg/day of VPA and 100 mg/kg/day of OXC. Ordinary drinking water was used as the control solution. The doses of drugs in treatment groups two, three, and four were defined according to the weights of the rats. Rats were weighted weekly and the drug doses were adjusted accordingly. The control solution and antiepileptics were administered orally in two divided doses with 12-h intervals for 90 days via gavage prepared specifically by bending the tip of a metal tube and coating it with silicon.

The VPA dose used was adopted from the study by Roste et al. (2002). The antiepileptic dose of OXC was proposed as 30 mg/kg for single use and higher for chronic use (Tecoma, 1999). We used the higher dose of 100 mg/kg/day in our study.

During the study period, one rat from group one, three rats from group two, two rats from group three, and four rats from group four were excluded from the study due to illnesses or death. At the end of the second month, the cell-cycle phases of animals were examined daily and the rats that were in the proestrous and diestrous phases of the estrous cycle were weighted and sacrificed 12–16 h after the last drug application. Intracardiac blood (6–8 ml) was obtained under anesthesia, and then the ovaries and uterus were extirpated and placed in a fixation solution. One hundred serial sections from each ovary were obtained and every 10, 20, 30, 40, 50, 60, 70, 80, 90, and 100 slides were chosen. These procedures were repeated for each dye.

For the endometrial tissue, terminal deoxynucleotidyl-transferase-mediated dUTP-biotin nick end-labeling (TUNEL)–staining protocols were applied on 5-μm paraffin tissue sections after 24–48 h. Slices were examined by two different researchers, and TUNEL-positive cells and eosinophil counts were noted. TUNEL-positive cells were counted among 100 cells detected by a 40× magnification from 10 regions randomly selected from 10 preparations. The preparations were also randomly obtained from the uterine tissues of each rat. The average of the TUNEL-positive cells was calculated for each rat. The eosinophil counts were also made by a 40× magnification within 10 randomly selected regions from 10 randomly selected preparations, and the average number of eosinophils was calculated for each rat.

Electron microscopic techniques

The ovarian and uterine tissues were placed in glutaraldehyde with 2.5% phosphate buffer. After evaluation of tissues with routine electron microscopy, they were embedded in Araldite. Slices with thickness of 1 μm were prepared from Araldite blocks via an LKB Lecia ultramicrotome (Leica, Wetzlar, Germany) and were stained with toluidine blue. The thick slices were evaluated with an Olympus BH2 photo light microscope (Olympus, Tokyo, Japan) and were photographed; these regions were marked and 0.5-μm thin slices were applied to the copper grids coated with Formvar (Monsanto Chemical Company, Creve Coeur, MO, U.S.A.). In order to obtain contrast, the slices were stained with uranyl acetate and lead citrate and they were evaluated and photographed with a Carl Zeiss EM 900 electron microscope (Carl Zeiss, Oberkochen,Germany).

TUNEL staining

TUNEL staining was applied in order to determine the number of apoptotic cells. The sections were stained with an in situ cell death detection kit (ApopTag Plus Peroxidase In Situ S7101, Lot: 0603025277; Chemicon International, Temecula, CA, U.S.A.). Slices (5 μm in thickness) were prepared from the paraffin blocks, which were produced for routine histologic specimen examination. The slices were incubated at 60°C for overnight. Sections were deparaffinized in xylene for an hour and rehydrated with reduced alcohol serials (100, 95, 85, 70, and 60%). The slices were incubated with 20 μg/ml of proteinase K for 10 min. Washing with phosphate-buffered saline (PBS) was performed in every stage. Endogenous peroxidase activity was blocked with 3% H_2O_2. After washing with PBS, the sections were incubated with equilibration buffer for 10–15 min and with terminal deoxynucleotidyl transferase (TdT) enzyme [77 μl reaction buffer + 33 μl TdT enzyme mix (1 μl TdT enzyme)] for 60 min at 37°C. Stop/wash buffer (1:10) was applied for 10 min at room

temperature, and the slices were incubated with anti-digoxigenin conjugate for 30 min. After washing with PBS 3 times for 5 min, the sections were stained with DAB components to detect TUNEL-positive cells and then they were counterstained with methyl green.

Statistical analysis

Data were analyzed with SPSS 11.5 program (SPSS Inc, Chicago, IL, U.S.A.). Descriptive statistics were given as the mean ± standard deviation (SD). The differences between the mean values of the experimental groups were studied with one-way analysis of variance (ANOVA). When the ANOVA results were significant, the Tukey honestly significant difference (HSD) test was applied, and the group or groups causing the differences were determined. The presence of statistically significant differences among the repeated measures within groups was examined with a dependent *t*-test when there were two repeated measures, and it was examined with repeated measures of ANOVA when there were more than two repeated measures. To determine the measure causing the difference, Bonferroni multiple comparison tests were used when repeated measures of ANOVA results were statistically significant. The statistical significance level was defined as $p < 0.05$.

Results

Results for the uterus

In the control group, the surface epithelial cells were observed to have a normal structure with a prismatic structure and euchromatic nuclei, which were located parallel to the long axis and the organelle content was appropriate for cell structure. At the apical surface of the cell, microvilli and cilia were clear. Intercellular junctions were distinct. Although mitochondria were distributed inside the cell, ger tubulus was active (Fig. 1A,B). Among the stromal cells, a few eosinophilic leukocytes were encountered (Fig. 1A). Stroma, with its cell and connective tissue features, was observed to have a normal structure.

In that VPA group, the surface epithelium had a slight disruption, which was conspicuous in the apical surface differentiation. Although intercellular junctions were normal, degenerative modifications were demonstrated in cell organelles. Mitochondrial swelling and cristolysis were observed. Another finding in the cytoplasm was the presence of large apoptotic particles. These particles, especially observed in apical cytoplasm, were thought to be formed as a result of phagocytosis of the apoptotic cells. The presence of primary and secondary lysosomes observed in the cells seemed to confirm this finding

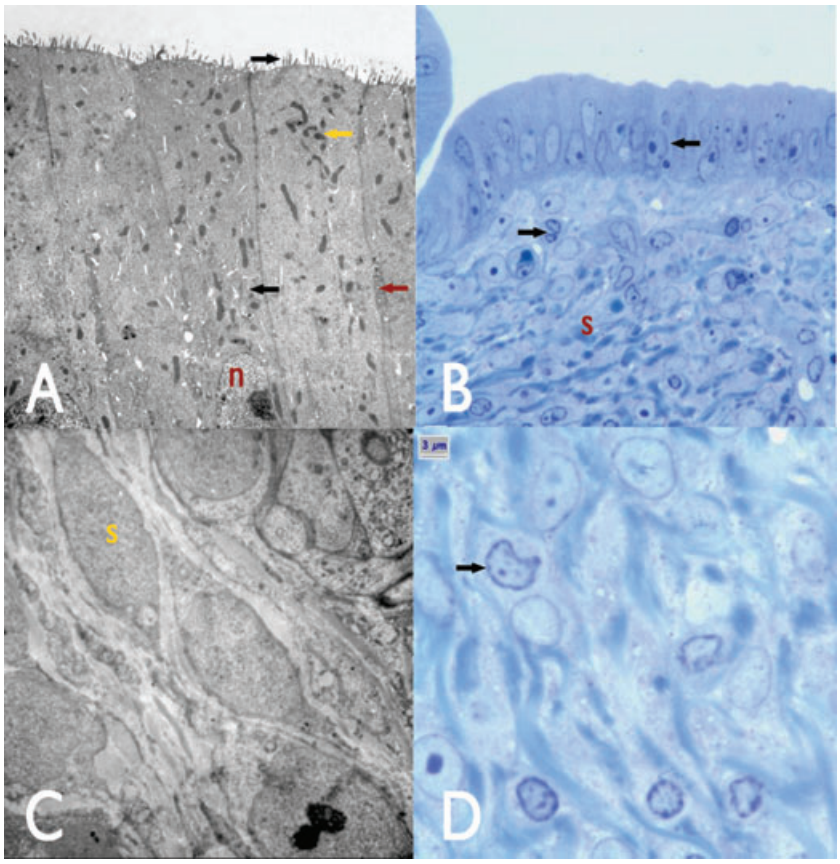


Figure 1.
(**A**) Normal structure of uterine epithelium in the control group. n, Nucleus; →, apical differentiations; red arrow, junctional complex; yellow arrow, mitochondrion; ←, ger tubulus (uranyl acetate-lead citrate x3,000). (**B**) Normal structure of uterine epithelium in control group. →, Eosinophil; ←, surface epithelial cells; s, stroma (toluidine blue x400). (**C**) Normal structure of stroma in control group. s, Stromal cell (uranyl acetate-lead citrate x3,000). (**D**) Normal structure of stroma in control group. →, Stromal cell (toluidine blue x1,000).
Epilepsia © ILAE

(Fig. 2A,B). Degeneration was observed in the stroma, particularly mitochondrial cristolysis at stromal cells. A slight swelling of the cells due to intracytoplasmic edema was observed. Although cell nuclei were normal in structure, prominent secondary lysosomes (phagosomes) were observed in a group of cells. In patches, the conversion of some cells into apoptotic particles was observed.

Some cells were observed to have apoptotic particles containing nuclear fragments and cytoplasmic content. It was thought that these apoptotic particles were phagocytosed by the stromal cells (Fig. 2C). Collagen fibers extended thoroughly as a bundle in the stroma. Increased eosinophilic infiltration was another finding observed in the stroma. Eosinophilic leukocytes bearing a great number of secretory granules were observed in the stroma (Fig. 2D,E).

In the OXC group, the epithelial cell surface differentiations, the nuclear structure, and the cell organelles were observed to be near-normal. Apoptotic particles containing cell cytoplasm and nuclear fragments in the apical cytoplasm were determined (Fig. 3A,B). The most evident modification in the stroma of the OXC group was the intracellular edema in stromal cells. Despite this, the cell nucleus was observed to have a normal structure. When ger tubulus were substantially active, mitochondrial cristolysis was apparent. An interesting finding was the presence of secondary lysosomes in some cells, whereas apoptotic particles were not observed in the stroma. Secondary lysosomes in some cells made groups in the cytoplasm. The collagen fibers were normal. A decrease in the number of eosinophilic leukocytes in the stroma was conspicuous (Fig. 3C,D).

In the VPA + OXC group, although some epithelial cells were observed to have normal structures, the presence of condensed cytoplasm in some cells and the finding of numerous apoptotic particles in the cytoplasm of these cells was interesting (Fig. 4A,B). In the VPA + OXC group, similar features with VPA and OXC groups were observed in the stromal cells. In addition, lots of apoptotic particles and secondary lysosomes were detected, as in the VPA group. The collagen fibers had normal structure. In

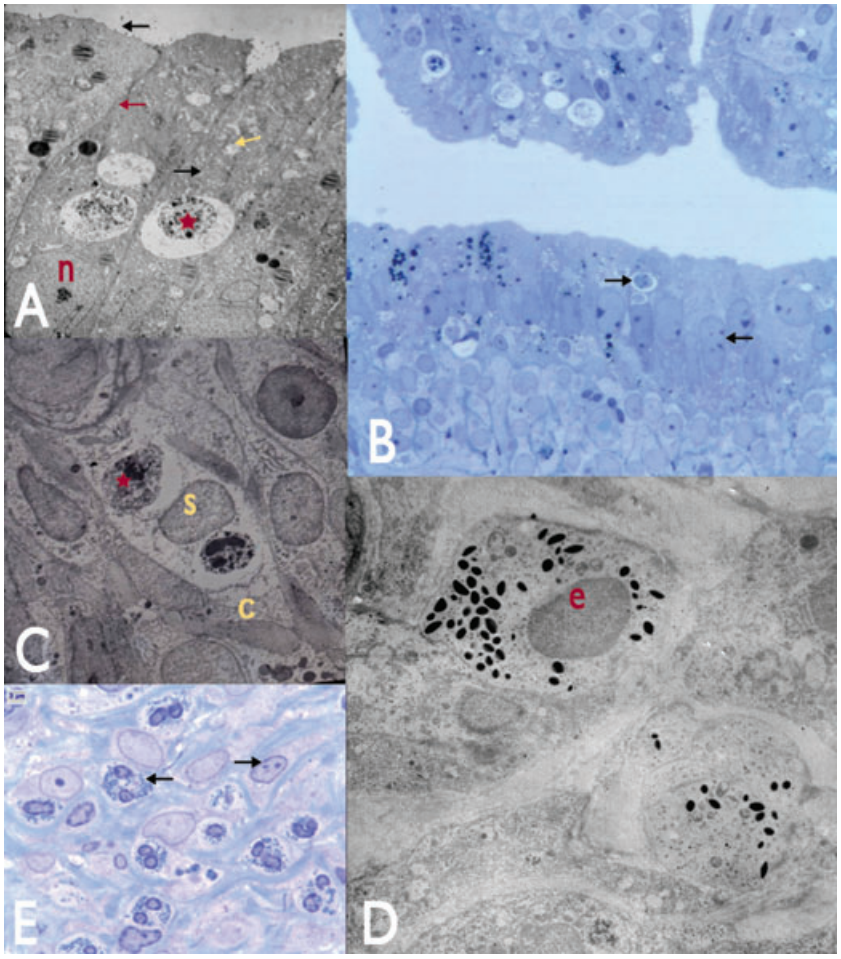


Figure 2.
(**A**) Uterine epithelium in the valproic acid (VPA) group. n, Nucleus; ←, apical differentiations; red arrow, junctional complex; yellow arrow, mitochondrion; →, ger tubulus; ★, apoptotic body (uranyl acetate-lead citrate x3,000). (**B**) Uterine epithelium in the VPA group. ←, Surface epithelial cells; →, apoptotic body (toluidine blue x400). (**C**) Stroma in the VPA group. s, Stromal cell; ★, apoptotic body; c, collagen fiber (uranyl acetate-lead citrate x7,000). (**D**) Stroma in the VPA group. e, Eosinophil (uranyl acetate-lead citrate x7,000). (**E**) Stroma in the VPA group. ←, Eosinophil; →, stromal cell (toluidine blue x1,000).
Epilepsia © ILAE

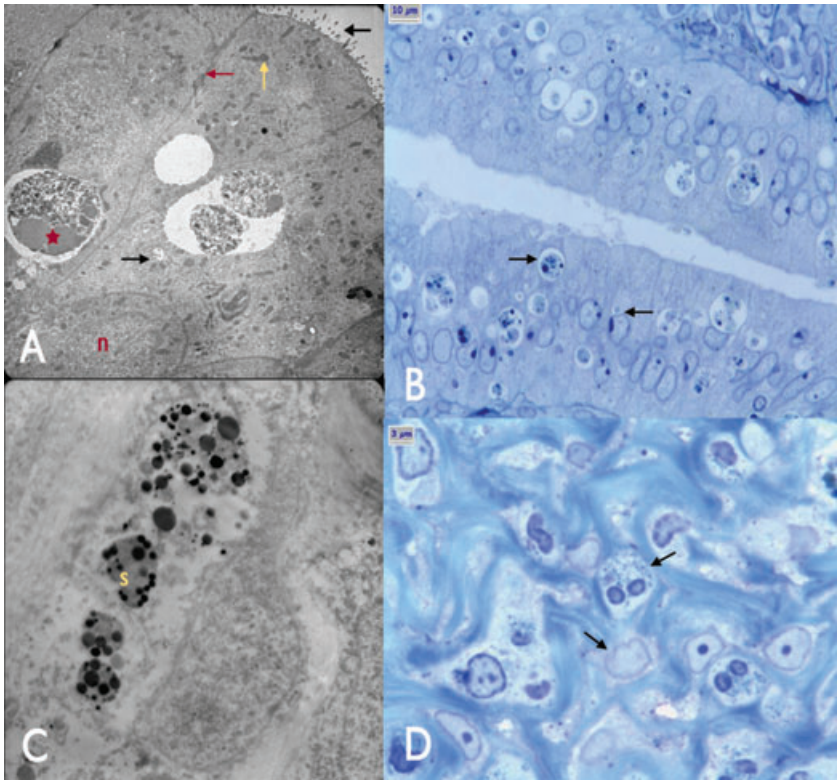


Figure 3.
(**A**) Uterine epithelium of the oxcarbazepine (OXC) group. n, Nucleus; ←, apical differentiations; red arrow, junctional complex; yellow arrow, mitochondrion; →, ger tubulus; ★, apoptotic body (uranyl acetate-lead citrate x3,000). (**B**) Uterine epithelium of the OXC group. ←, Surface epithelial cells; →, apoptotic body (toluidine blue x400). (**C**) Stroma of the OXC group. s, Secondary lysosome (uranyl acetate-lead citrate x7,000). (**D**) Stroma of the OXC group. ←, Eosinophil; →, stromal cell (toluidine blue x1,000).
Epilepsia © ILAE

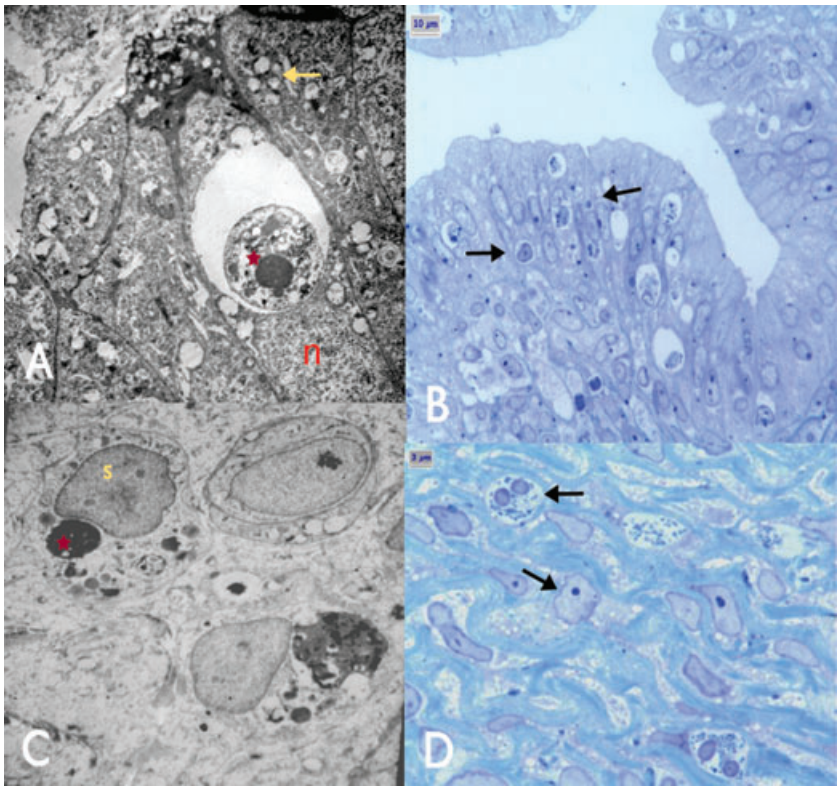


Figure 4.
(**A**) Uterine epithelium of the oxcarbazepine and valproic acid (OXC + VPA) group. n, Nucleus; yellow arrow, mitochondrial cristolysis; ★, apoptotic body (uranyl acetate-lead citrate x3,000). (**B**) Uterine epithelium of the VPA + OXC group. ←, Surface epithelial cells; →, apoptotic body (toluidine blue x400). (**C**) Stroma of the OXC + VPA group. s, Stromal cell; ★, apoptotic body; (uranyl acetate-lead citrate x7,000). (**D**) Stroma of the VPA + OXC group. ←, eosinophil; →, stromal cell (toluidine blue x1,000).
Epilepsia © ILAE

the stroma, eosinophilic infiltration, including secretory granules, were detected less often than the VPA group, and more often than the OXC and control groups (Fig. 4C,D).

Results for ovary

In the control group, the granulosa cells were edematous, and widespread cristolysis was observed in the mitochondria, considering the follicles were in the late graft stage. Ger tubulus were substantially active (Fig. 5A). A group of cells was observed in the metaphase stage of mitosis (Fig. 5B).

In the VPA group, apoptotic particles rich in lipid content drew attention, especially in the cytoplasm of the cells constituting the basal and middle layers of the follicle (Fig. 5C). The conversion of a group of cells into apoptotic particles was observed. However, the top layer cells were similar with the control group in terms of both the organelle and nuclear structures (Fig. 5D).

In the OXC group, the most evident electron microscopic modification in the basal and middle layer cells of the follicle was the presence of granulosa cells with light- and dark-colored cytoplasm. Chromatin condensation was apparent in the nucleus of the cells containing dark-colored cytoplasm, and this observation was accepted as an indication of cell apoptosis (Fig. 6A). The cells containing light-colored cytoplasm were also hypertrophic, displaying intracytoplasmic edema, and disruption of organelle structure was observed (Fig. 6B). When the top layer cells adjacent to the follicular fluid were observed, a similarity with the previous group was determined. Although there

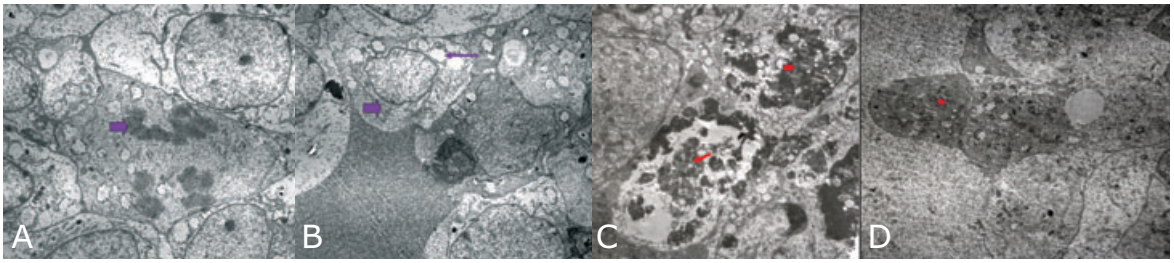


Figure 5.
(**A**) Ovarian tissue of the control group. ➡, Mitochondrial crystolysis; ➡, active ger tubulus (uranyl acetate-lead citrate x3,000). (**B**) Ovarian tissue of the control group. ➡, Metaphase stage of mitotic division (uranyl acetate-lead citrate x3,000). (**C**) Ovarian tissue of the valproic acid (VPA)–treated group. ➡, Apoptotic particles rich in terms of lipid content; ➡, cell becoming apoptotic particles (uranyl acetate-lead citrate x3,000). (**D**) Ovarian tissue of the VPA-treated group. ★, Top layer cells (uranyl acetate-lead citrate x3,000).
Epilepsia © ILAE

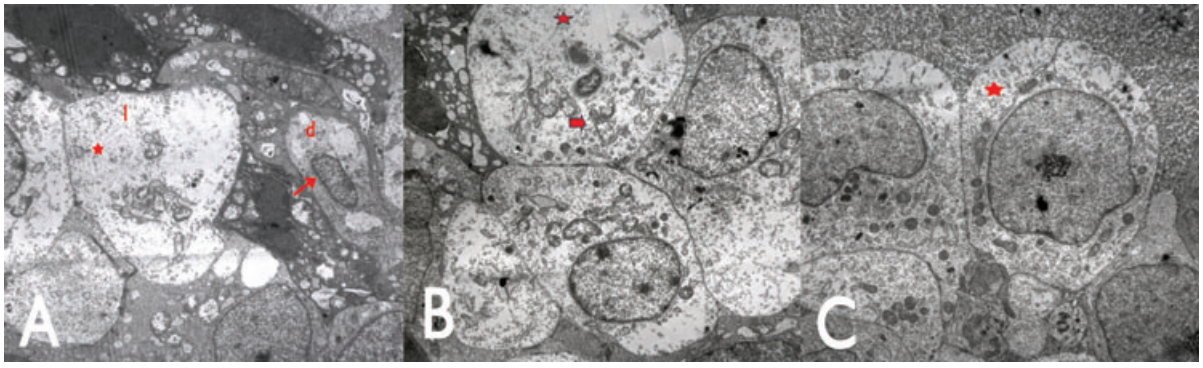


Figure 6.
(**A**) Ovarian tissue of the oxcarbazepine (OXC)–treated group. l, Light cells; d, dark cells; ➡, chromatin condensation in dark cells; ★, hypertrophy in light cells (uranyl acetate-lead citrate x3,000). (**B**) Ovarian tissue of the OXC-treated group. ★, Intracytoplasmic edema in light cells; ➡, deformation in organelle orientation (uranyl acetate-lead citrate x3,000). (**C**) Ovarian tissue of the OXC-treated group. ★, Intracytoplasmic edema in apical cells (uranyl acetate-lead citrate x3,000).
Epilepsia © ILAE

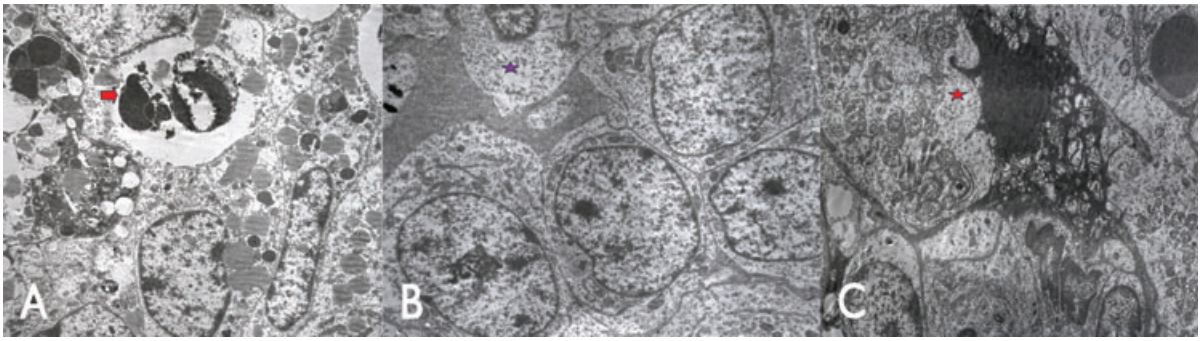


Figure 7.
(**A**) Ovarian tissue of the valproic acid and oxcarbazepine (VPA + OXC)–treated group. ➡, Apoptotic particles (uranyl acetate-lead citrate x3,000). (**B**) Ovarian tissue of the VPA + OXC–treated group. ★, Intracytoplasmic edema (uranyl acetate-lead citrate x3,000). (**C**) Ovarian tissue of the VPA + OXC–treated group. ★, Intracytoplasmic edema in apical cells (uranyl acetate-lead citrate x4,400).
Epilepsia © ILAE

were patches of intracytoplasmic edema, the content of the organelle and nuclear structure was observed as normal (Fig. 6C).

In VPA and OXC groups, degenerative modifications caused by both agents were observed. In the basal and middle layer cells, although the cells transformed to apoptotic particles were observed as in VPA group, cells with electron-dense cytoplasm having pyknotic nuclei were observed in patches, as in the OXC group (Fig. 7A). In this group, hypertrophic cells and intracytoplasmic edema were also observed (Fig. 7B). The appearance of the layer cells adjacent to the follicle fluid were similar to the OXC group, and although the nuclear and organelle content was normal, intracytoplasmic edema was observed in the cells (Fig. 7C).

TUNEL staining

In uterus, the number of TUNEL-positive luminal epithelial cells was 7.20 ± 1.32 in control group, and it significantly increased to 29.60 ± 1.58, 34.20 ± 2.53, and 54.80 ± 2.04 in the VPA, OXC, and VPA + OXC groups, respectively ($p < 0.001$). The number of TUNEL-positive glandular epithelium cells was also highest in the VPA + OXC group (42.10 ± 1.66) compared to the control (3.50 ± 1.08), VPA (13.90 ± 1.37), and OXC (22.00 ± 2.31) groups. Contrary to these results, the number of TUNEL-positive stroma cells was 12.60 ± 1.51 in the control group, and the highest increase was observed in the VPA group (30.30 ± 1.49). There was a statistically significant difference between the number of TUNEL-positive stroma cells of the OXC (19.90 ± 2.18) and the

Table 1. TUNEL-staining findings of the luminal epithelium, glandular epithelium, and stroma in the uterus

Number of TUNEL-positive cells	Group 1 (Control)	Group 2 (VPA)	Group 3 (OXC)	Group 4 (VPA + OXC)	p-value[a]
Luminal epithelium	7.20 ± 1.32	29.60 ± 1.58[b]	34.20 ± 2.53[b,c]	54.80 ± 2.04[b,c,d]	<0.001
Glandular epithelium	3.50 ± 1.08[e]	13.90 ± 1.37[b,e]	22.00 ± 2.31[b,c,e]	42.10 ± 1.66[b,c,d,e]	<0.001
Stroma cells	12.60 ± 1.51[e,f]	30.30 ± 1.49[b,f]	19.90 ± 2.18[b,c,e]	14.50 ± 2.84[c,d,e,f]	<0.001
p-value[g]	<0.001	<0.001	<0.001	<0.001	

Data are presented as mean ± standard deviation (SD).
VPA, valproic acid; OXC, oxcarbazepine.
[a]One-way analysis of variance (ANOVA).
[b]$p < 0.001$ versus control group.
[c]$p < 0.001$ versus VPA group.
[d]$p < 0.001$ versus OXC group.
[e]$p < 0.001$ versus lumen epithelium.
[f]$p < 0.001$ versus glandular epithelium.
[g]Repeated measures of ANOVA.

Table 2. Eosinophil counts of endometrial stroma in experimental groups

	Group 1 (Control)	Group 2 (VPA)	Group 3 (OXC)	Group 4 (VPA + OXC)	p-value[a]
Eosinophil infiltration in stroma	1.1 ± 0.74	18.0 ± 1.15[b]	5.1 ± 0.88[b,c]	9.0 ± 1.49[b,c,d]	<0.001

Data are presented as mean ± standard deviation (SD).
VPA, valproic acid; OXC, oxcarbazepine.
[a]One-way analysis of variance (ANOVA).
[b]$p < 0.001$ versus control group.
[c]$p < 0.001$ versus VPA group.
[d]$p < 0.001$ versus OXC group.

control groups, whereas no significant difference was observed between the VPA + OXC (14.50 ± 2.84) and the control groups (Table 1).

Eosinophil counts

The highest number of eosinophils in the stroma was found in the VPA group. The difference in the eosinophil counts between the control and the other groups was statistically significant ($p < 0.001$) (Table 2).

Discussion

In the present study, the effects of two AEDs, VPA and OXC, on rat uterine and ovarian cells were investigated. In uterus, VPA induced apoptosis in the stroma and caused mitochondrial swelling and cristolysis; however, OXC had negative effects on epithelial cells and led to intracellular edema. In the ovarian tissue, VPA and OXC increased apoptosis and in the OXC treated group, in addition to the apoptotic particles, intracytoplasmic edema and disruption of organelle structure were observed. The negative effects on the uterine and ovarian cells were more conspicuous when two drugs were applied together.

In transmission electron microscopy (TEM) studies performed on different cells, the negative effects of VPA on shape, size, and number of mitochondria were demonstrated (Neuman et al., 2001). Loss of mitochondrial cristae and a decrease in the mitochondrial matrix in human hepatoblastoma cells were determined by Neuman et al. (2001). An increase in lipid droplets was also determined in these cells. Meanwhile, the research demonstrated the apoptotic effect of VPA on hepatocytes (Neuman et al., 2001). In addition, VPA acts through microvascularization (vasogenic effect) at the blood–brain barrier and causes astroglial damage (Sobaniec-Lotowska, 2003). Similarly, prenatal VPA application affected specific transport functions of glucose in the microvascular endothelium (Vorbrodt et al., 2005). Chen et al. (2007) found that VPA induces apoptosis of microglia cells and that the apoptosis of microglia was accompanied by disruption of the mitochondrial membrane potential. Miyatake et al. (2007) suggested that VPA affects membrane trafficking, which leads to enhanced sensitivity to cell-wall damage in fission yeast.

The morphologic studies investigating the effects of OXC on cells are limited. Degeneration and edema of the hippocampal neurons have been demonstrated with OXC usage (Araujo et al., 2004). In this study, immunocytochemical staining was performed and changes in mitochondrial membrane potential were detected. As a result of this study, it was shown that OXC causes a decrease in the mitochondrial membrane potential (Araujo et al., 2004).

The present study demonstrated that VPA causes mitochondrial swelling and cristolysis, especially in the stromal cells of the uterus. This result indicates that VPA disrupts the mitochondria and confirms the contraindication of VPA in mitochondrial diseases. OXC has negative effects on uterine epithelial cells and causes intracytoplasmic edema. A decrease in the number of eosinophilic leukocytes in the stroma was conspicuous. The reason for the intracytoplasmic edema might be the decrease in ATP levels (Araujo et al., 2004). Water enters into the cell due to high intracellular sodium levels (hyperosmolar). This condition might explain the hyponatremia related to OXC and edema in the cell. Another probable cause of the hyponatremia is an increase in arginine vasopressin (AVP). AVP is thought to be the most important underlying mechanism of CBZ-related hyponatremia via direct or kidney tubular mechanisms (Isojarvi et al., 2001).

In uterus, TUNEL-staining was applied in order to determine the number of apoptotic cells. In the present study, it was found that the number of TUNEL-positive luminal epithelium cells significantly increased in the VPA, OXC, and VPA + OXC treated groups. The increase in the number of TUNEL-positive glandular epithelium cells was also significant for the VPA, OXC, and VPA + OXC groups. These findings demonstrated that both VPA and OXC act as apoptotic agents in the luminal and glandular epithelium of the uterus. Our previous results also described the apoptotic characteristics of VPA and OXC on ovarian follicles (Cansu et al., 2008). The highest increase in the number of TUNEL-positive stromal cells was observed in VPA group, and although OXC

also significantly increased TUNEL-positive cells, there was no statistically significant difference between VPA + OXC and control groups in terms of TUNEL-positive stroma cells. Histone deacetylase (HDAC) inhibitors suppress proliferation of endometrial stromal cells through induction of cell cycle arrest and apoptosis as well (Wu & Guo, 2008). VPA, with HDAC inhibitory activity, enhanced the antiestrogen action by promoting cell death via apoptosis without affecting cell cycling on uterine endometrial cells (Hodges-Gallagher et al., 2007). It can be concluded that the negative effect of VPA and OXC on stroma cells is reduced when these two drugs are applied together. VPA was shown to decrease the number of follicles in our previous study (Cansu et al., 2008), and this may be due to the HDAC inhibitor activity of VPA with the induction of cell cycle arrest.

VPA-treated mice were observed to have up to a 30-fold increase in the number of TUNEL-positive cells in the external granule cells of the cerebellum (Yochum et al., 2008). In our previous study, VPA increased the apoptotic cells in the ovary (Cansu et al., 2008). In the present study, apoptotic particles rich in lipid content and conversion of a group of cells into apoptotic particles were observed.

Cell apoptosis in the ovary was also determined in the OXC group by means of observation of nuclear chromatin condensation. In a study investigating the neurotoxic and neuroprotective effects of some AEDs, it was demonstrated that, treatment with AEDs, mainly carbamazepine and oxcarbazepine, caused nuclear chromatin condensation in some neurons, which was characteristic of apoptosis (Ambrosio et al., 2000). In addition, intracytoplasmic edema and organelle structure disruption in granulosa cells were observed in the present study. This can be due to the entrance of sodium into the cell with fluid, which might cause intracytoplasmic edema and disruption in organelle structure.

When VPA and OXC were applied together, both intracytoplasmic edema and apoptotic particles that were rich in lipid content were observed. Therefore, degenerative characteristics and toxicity increased in the VPA + OXC group. In the present study, it was determined that the use of both drugs together led to the same total of effect changes in the cell as when these drugs were used separately. Therefore, it was considered that the toxic effects on the cell were performed by different mechanisms.

Eosinophils play an important role in the pathogenesis of late-type inflammatory reactions and are absent from the normal endometrium (Bousquet et al., 1990). Klebanoff reported that eosinophils were involved in endometrial tissue breakdown through their degranulation and release of cytotoxic proteins and superoxide molecules (Klebanoff, 1965). In another study performed on rats, it was observed that the pinealectomy led to a decrease in embryo implantation. The presence of eosinophils was observed in the endometria of the rats (Dair et al., 2008). In the present study, the number of eosinophils in endometrial tissue was highest in the VPA group. As a result, VPA might cause abortion by preventing implantation of the embryo in the uterus. Higher doses of VPA can entail a greater risk for spontaneous abortion and fetal malformations (Vajda & Eadie, 2005). In a group of pregnant women taking VPA, supplementation with folic acid had significant benefits on spontaneous abortion, since VPA interferes with folate metabolism (Pittschieler et al., 2008). OXC also increases eosinophil numbers compared to the control group; however, when treated with VPA, OXC might have a protective effect due to the decrease in the number of eosinophils in the VPA + OXC group.

The present study demonstrated that VPA caused mitochondrial cristolysis and OXC caused intracytoplasmic edema; therefore, VPA and OXC trigger both apoptotic and degenerative periods. Furthermore, VPA prevents implantation of embryo to the uterus and may cause abortion via endometrial eosinophil infiltration.

As stated in some of the previous studies, morphologic studies demonstrated the effect of VPA; however, they could not provide underlying molecular mechanisms to be understood clearly (Vorbrodt et al., 2005). Studies, especially utilizing quantitative genetic and molecular biology methods, are required to understand these mechanisms.

Acknowledgments

This study has been awarded by ''Research Support Award'' by Bayindir Hospital in 2006. We thank Bayindir Hospital for financial support. We also thank Prof. E. Calguner from Department of Anatomy, Faculty of Medicine, Gazi University, Ankara for his help while using the animal lab where he works as a manager.

We confirm that we have read the Journal's position on issues involved in ethical publication and affirm that this report is consistent with those guidelines.

Disclosure: None of the authors has any conflict of interest to disclose.

References

Ambrosio AF, Silva AP, Araujoa I, Malva JO, Soares-da-Silva P, Carvalho AP, Carvalho CM. (2000) Neurotoxic/neuroprotective profile of carbamazepine, oxcarbazepine and two new putative antiepileptic drugs, BIA 2-093 and BIA 2-024. *Eur J Pharmacol* 406:191–201.

Araujo IM, Ambrosio AF, Leal EC, Verdasca MJ, Malva JO, Soares-da-Silva P, Carvalho AP, Carvalho CM. (2004) Neurotoxicity induced by antiepileptic drugs in cultured hippocampal neurons: a comparative study between carbamazepine, oxcarbazepine, and two new putative antiepileptic drugs, BIA 2-024 and BIA 2-093. *Epilepsia* 45:1498–1505.

Bousquet J, Chanez P, Lacoste JY, Barneon G, Ghavanian N, Enander I, Venge P, Ahlstedt S, Simony-Lafontaine J, Godard P. (1990) Eosinophilic inflammation in asthma. *N Engl J Med* 323:1033–1039.

Cansu A, Giray SG, Serdaroglu A, Erdogan D, Coskun ZK, Korucuoglu U, Biri AA. (2008) Effects of chronic treatment with valproate and oxcarbazepine on ovarian folliculogenesis in rats. *Epilepsia* 49:1192–1201.

Chen PS, Wang CC, Bortner CD, Peng GS, Wu X, Pang H, Lu RB, Gean PW, Chuang DM, Hong JS. (2007) Valproic acid and other histone deacetylase inhibitors induce microglial apoptosis and attenuate lipopolysaccharide-induced dopaminergic neurotoxicity. *Neuroscience* 149:203–212.

Dair EL, Simoes RS, Simoes MJ, Romeu LR, Oliveira-Filho RM, Haidar MA, Baracat EC, Soares JM Jr. (2008) Effects of melatonin on the endometrial morphology and embryo implantation in rats. *Fertil Steril* 89:1299–1305.

Emmanouil-Nikoloussi EN, Foroglou NG, Kerameos-Foroglou CH, Thliveris JA. (2004) Effect of valproic acid on fetal and maternal organs in the mouse: a morphological study. *Morphologie* 88: 41–45.

Hodges-Gallagher L, Valantine CD, Bader SE, Kushner PJ. (2007) Inhibition of histone deacetylase enhances the anti-proliferative action of antiestrogens on breast cancer cells and blocks tamoxifen-induced proliferation of uterine cells. *Breast Cancer Res Treat* 105:297–309.

Isojarvi JI, Huuskonen UE, Pakarinen AJ, Vuolteenaho O, Myllyla VV. (2001) The regulation of serum sodium after replacing carbamazepine with oxcarbazepine. *Epilepsia* 42:741–745.

Klebanoff SJ. (1965) Inactivation of estrogen by rat uterine preparations. *Endocrinology* 76:301–311.

Miyatake M, Kuno T, Kita A, Katsura K, Takegawa K, Uno S, Nabata T, Sugiura R. (2007) Valproic acid affects membrane trafficking and cell-wall integrity in fission yeast. *Genetics* 175: 1695–1705.

Neuman MG, Shear NH, Jacobson-Brown PM, Katz GG, Neilson HK, Malkiewicz IM, Cameron RG, Abbott F. (2001) CYP2E1-mediated modulation of valproic acid-induced hepatocytotoxicity. *Clin Biochem* 34:211–218.

Pittschieler S, Brezinka C, Jahn B, Trinka E, Unterberger I, Dobesberger J, Walser G, Auckenthaler A, Embacher N, Bauer G, Luef G (2008) Spontaneous abortion and the prophylactic effect of folic acid supplementation in epileptic women undergoing antiepileptic therapy. *J Neurol* 255:1926–1931.

Roste LS, Tauboll E, Isojarvi JI, Pakarinen AJ, Huhtaniemi IT, Knip M, Gjerstad L. (2002) Effects of chronic valproate treatment on reproductive endocrine hormones in female and male Wistar rats. *Reprod Toxicol* 16:767–773.

Seegmiller RE, Harris C, Luchtel DL, Juchau MR. (1991) Morphological differences elicited by two weak acids, retinoic and valproic, in rat embryos grown in vitro. *Teratology* 43:133–150.

Sobaniec-Lotowska ME. (2003) Ultrastructure of astrocytes in the cortex of the hippocampal gyrus and in the neocortex of the temporal lobe in experimental valproate encephalopathy and after valproate withdrawal. *Int J Exp Pathol* 84:115–125.

Tecoma ES. (1999) Oxcarbazepine. *Epilepsia* 40:S37–S46.

Vajda FJ, Eadie MJ. (2005) Maternal valproate dosage and feotal malformations. *Acta Neurol Scand* 112:137–143.

Vorbrodt AW, Dobrogowska DH, Kozlowski PB, Rabe A, Tarnawski M, Lee MH. (2005) Immunogold study of effects of prenatal exposure to lipopolysaccharide and/or valproic acid on the rat blood–brain barrier vessels. *J Neurocytol* 34:435–446.

Wu Y, Guo SW. (2008) Histone deacetylase inhibitors trichostatin A and valproic acid induce cell cycle arrest and p21 expression in immortalized human endometrial stromal cells. *Eur J Obstet Gynecol Reprod Biol* 137:198–203.

Yochum CL, Dowling P, Reuhl KR, Wagner GC, Ming X. (2008) VPA-induced apoptosis and behavioral deficits in neonatal mice. *Brain Res* 1203:126–132.